6

Lipid Metabolic Dysregulation in Traumatic Chronic Subdural Hematoma: An Integrated Plasma-Hematoma Metabolomic Profiling and Machine Learning Approach Identifies an 11-Metabolite Diagnostic Signature Xiang Mao¹

The author has chosen not to publish their abstract

¹ the First Affiliated Hospital of Anhui Medical University

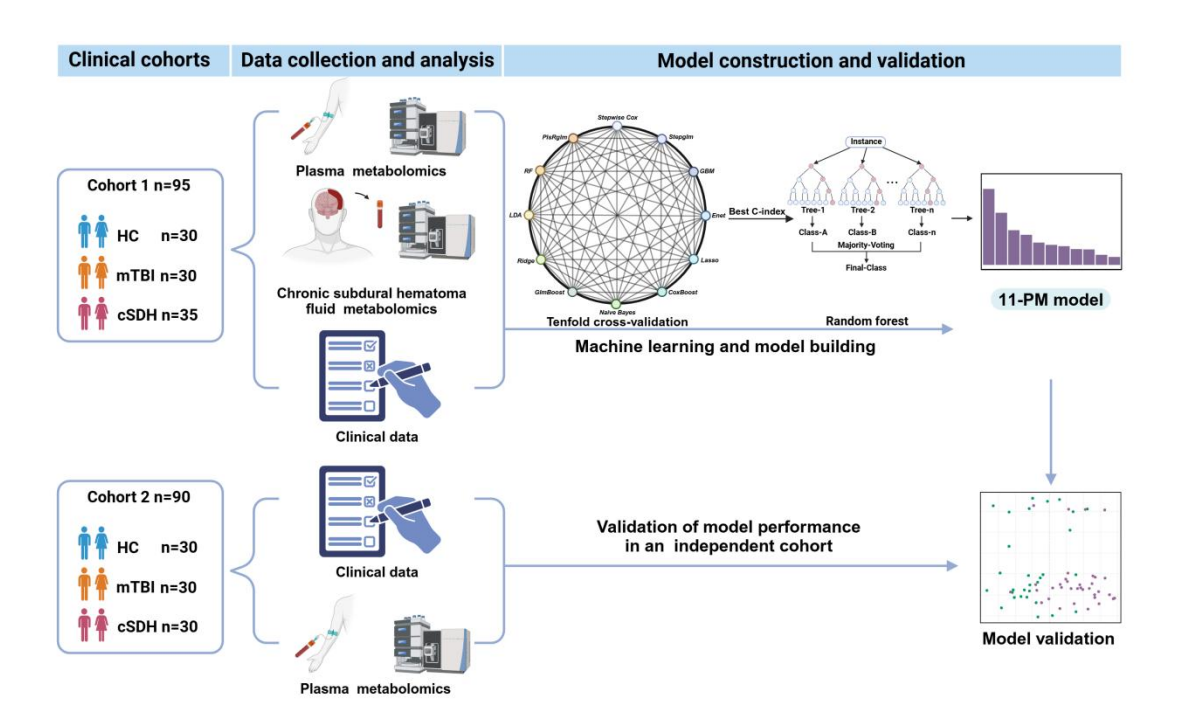


Figure 1 Flow chart of the experimental design.

Totally 185 plasma samples and 35 subdural hematoma fluid samples were collected for metabolomics analysis. The metabolic profiles of chronic subdural hematoma (cSDH) patients and mild traumatic brain injury (mTBI) patients in Cohort 1 were compared to depict the metabolic reprogramming in cSDH. Using the metabolomics data from Cohort 1 and machine learning techniques, a diagnostic model for cSDH (11-PM model) was created and validated. This model was further verified in the validation Cohort 2. The illustration was created with a full license on BioRender.com.

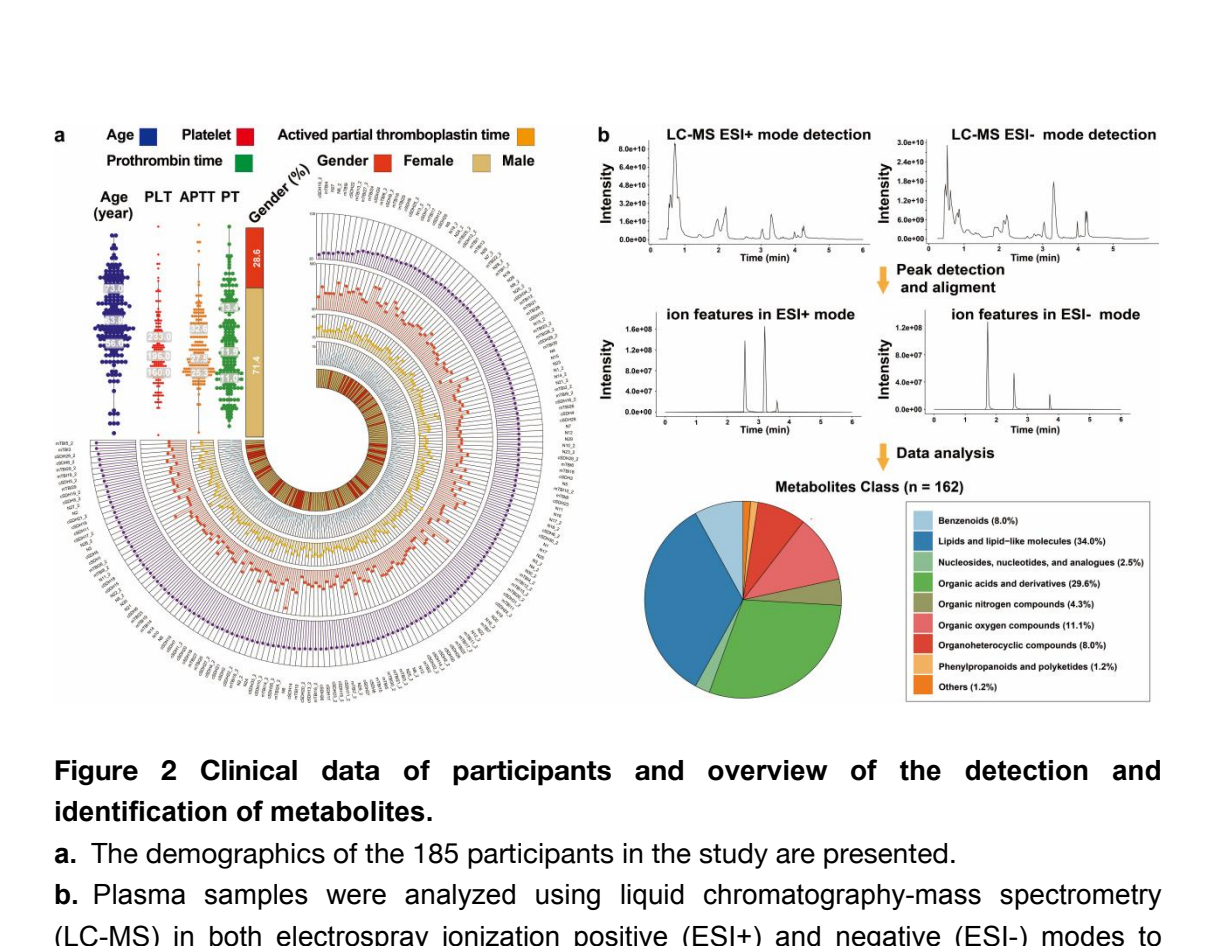


Figure 2 Clinical data of participants and overview of the detection and

- a. The demographics of the 185 participants in the study are presented.
- b. Plasma samples were analyzed using liquid chromatography-mass spectrometry (LC-MS) in both electrospray ionization positive (ESI+) and negative (ESI-) modes to enhance the ionization and detection of alkaline and acidic compounds, respectively. After peak detection, alignment and metabolite identification, a total of 162 metabolites were confidently annotated. This dual-mode analytical strategy ensured comprehensive coverage of the plasma metabolome, facilitating the detection of a wide array of metabolic features.

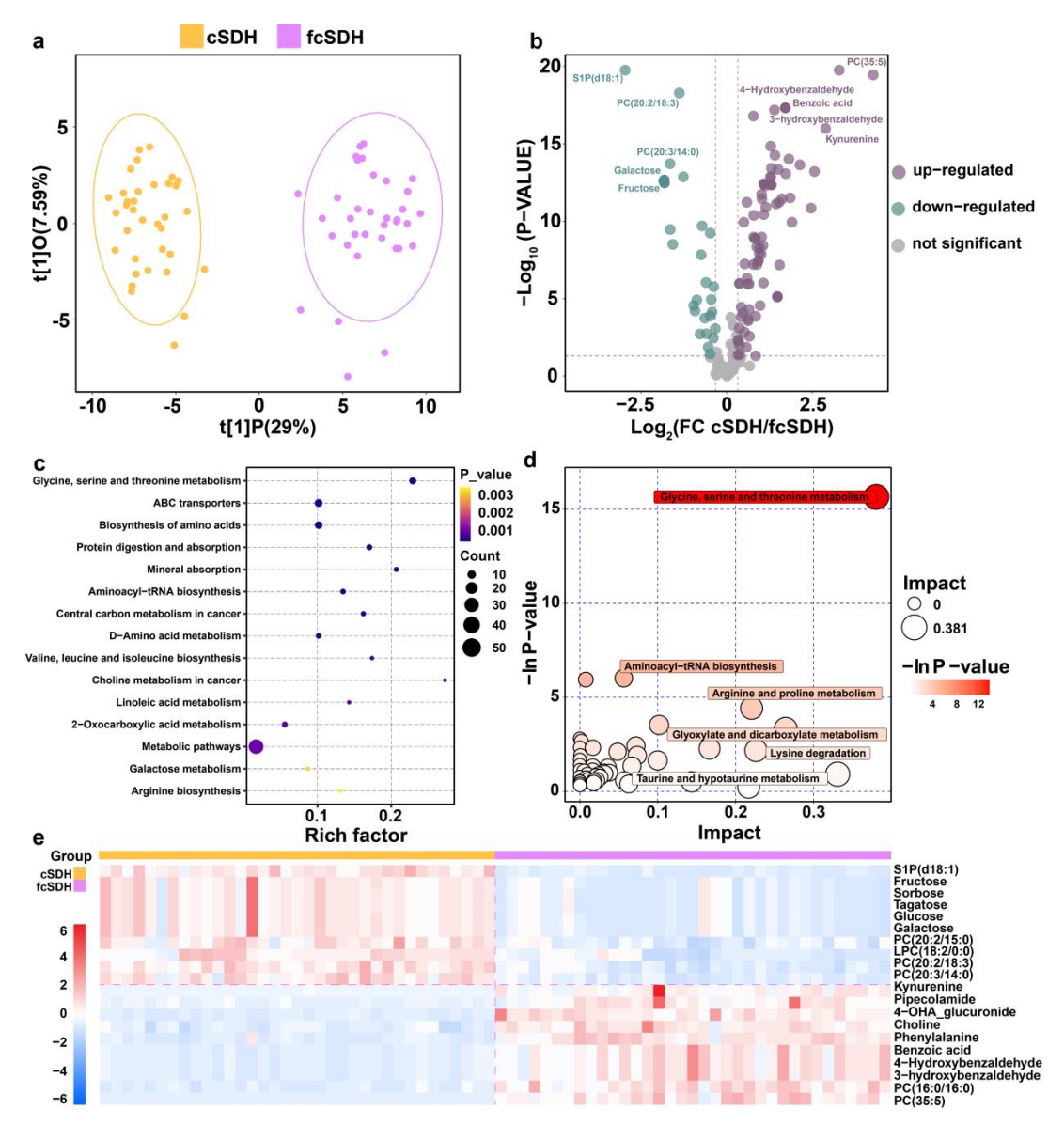


Figure 3 Metabolomic changes in plasma and subdural fluid in cSDH patients.

- **a.** Principal Component Analysis (PCA) of Cohort 1 metabolomics data comparing plasma (colored in yellow) and subdural fluid (colored in red) in cSDH patients.
- **b.** Volcano plot of the detected metabolites in metabolomics comparing plasma and subdural fluid in cSDH patients. Significantly differential metabolites are colored in purple (upregulated) and green (downregulated); the others are colored in gray.
- **c.** Kyoto Encyclopedia of Genes and Genomes (KEGG) metabolic pathways enriched by significantly differential metabolites between plasma and subdural fluid in cSDH patients.
- **d.** Pathway analysis of significantly differential metabolites between plasma and subdural fluid in cSDH patients.
- **e.** Heat map of major differential metabolites between plasma and subdural fluid in cSDH patients.

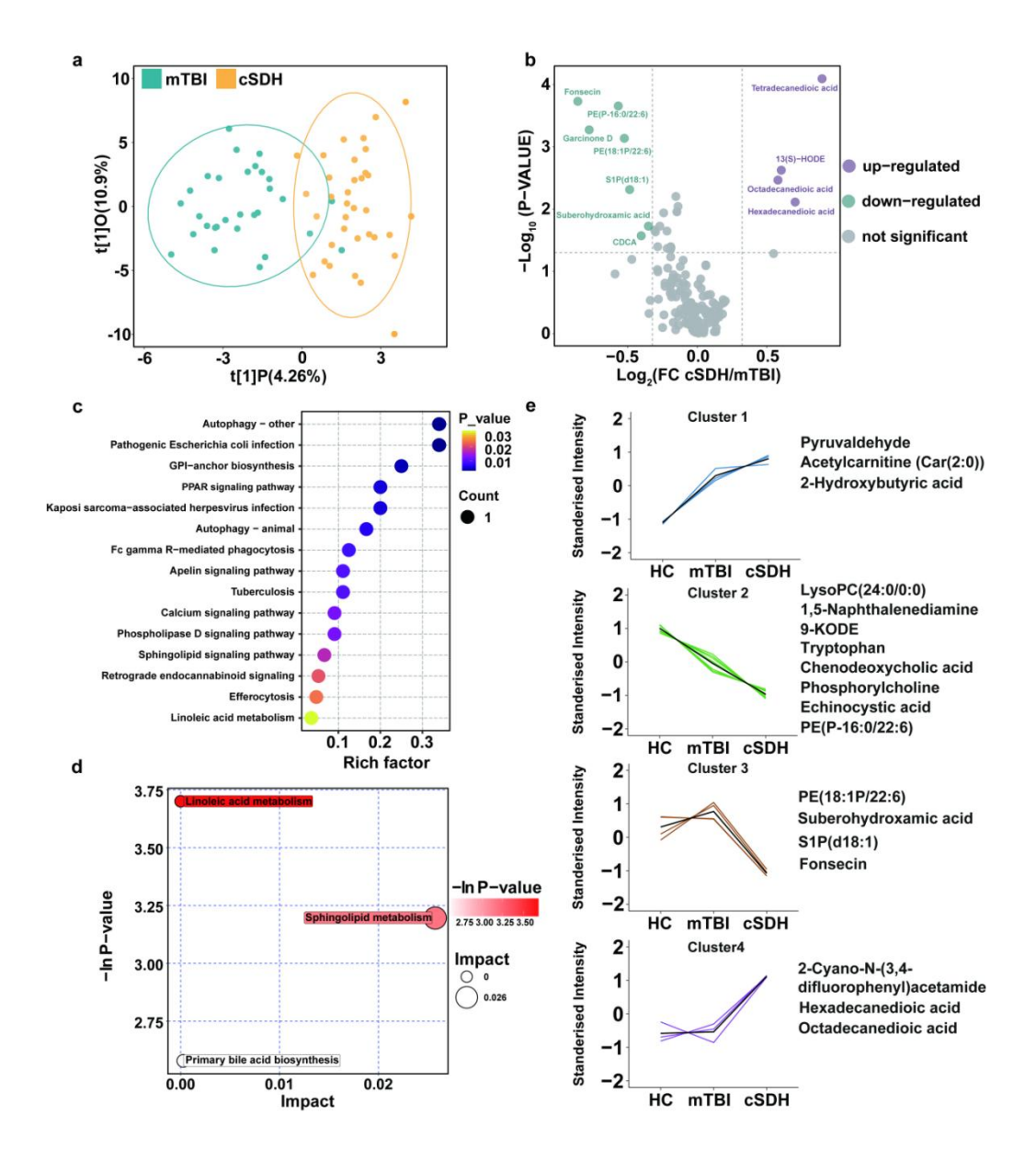


Figure 4 Reprogrammed plasma metabolic landscape of cSDH patients compared with mTBI patients.

- **a.** PCA of Cohort 1(n = 65) plasma metabolomics data comparing cSDH patients (colored in yellow) and mTBI patients (colored in green).
- **b.** Volcano plot of the detected metabolites in Cohort 1 plasma metabolomics (cSDH group versus mTBI group). Significantly differential metabolites are colored in purple (upregulated) and green (downregulated); the others are colored in gray.
- **c.** KEGG metabolic pathways enriched by significantly differential metabolites between cSDH and mTBI group.
- **d.** Pathway analysis of significantly differential metabolites between cSDH and mTBI group.
- **e.** Mfuzz clustering of metabolic trajectories using the differential metabolites according to the metabolic changes' similarity in Cohort 1. Representative metabolites of each cluster are presented on the side.

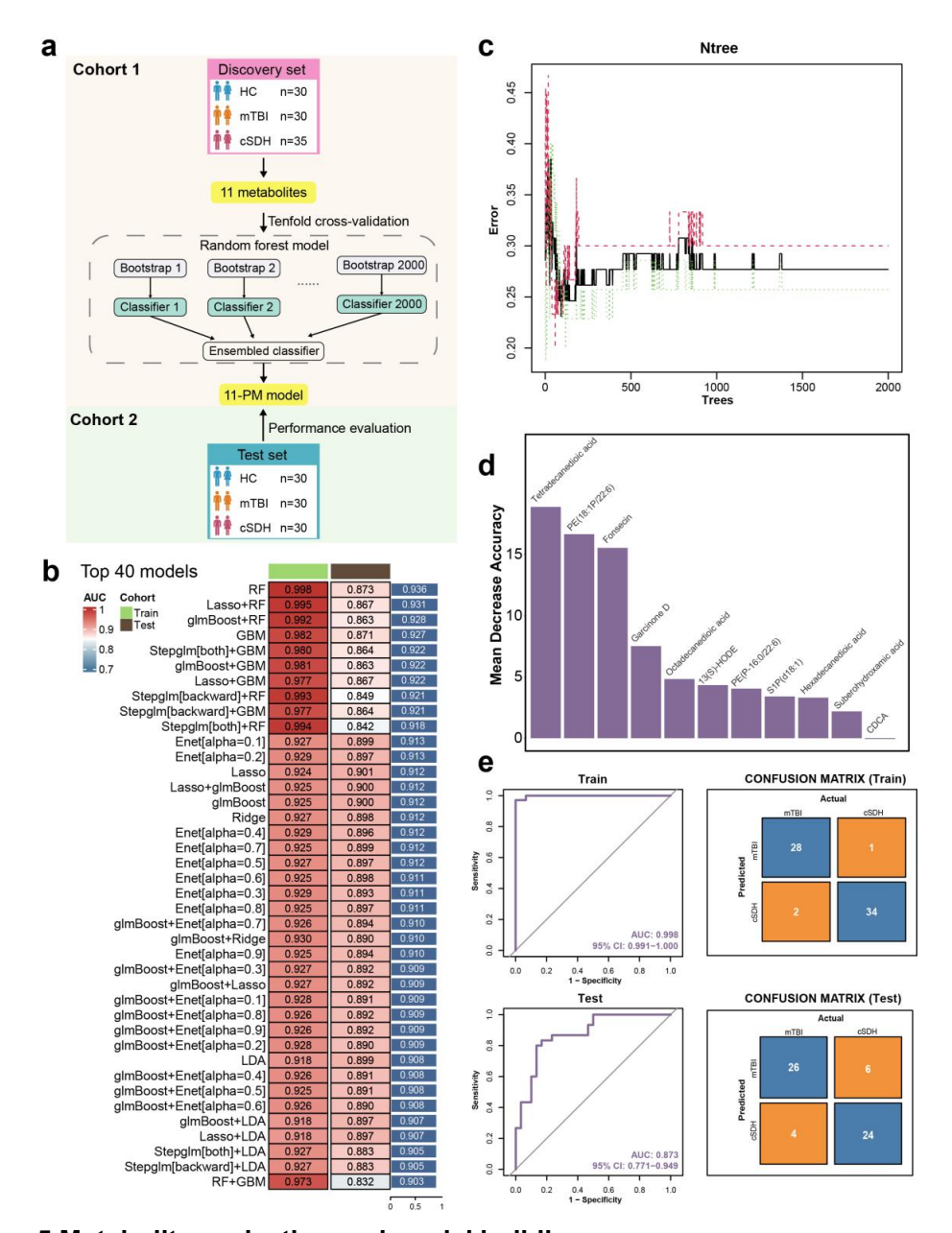
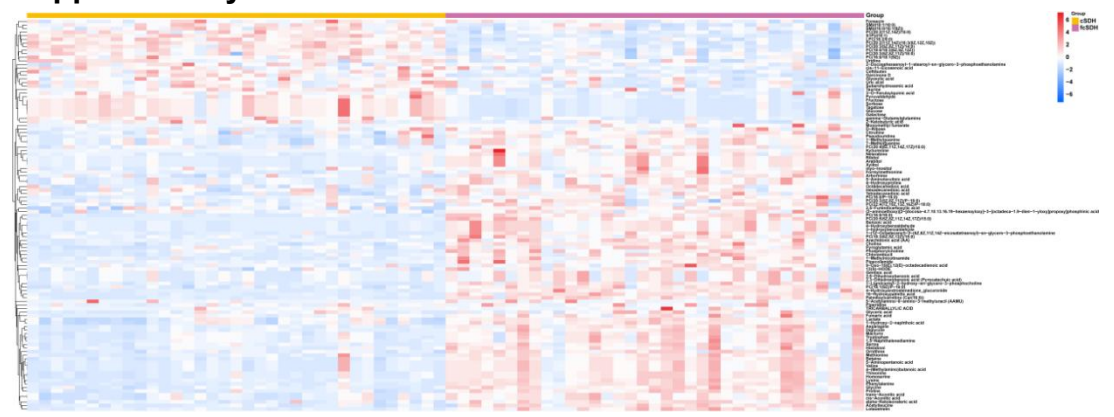


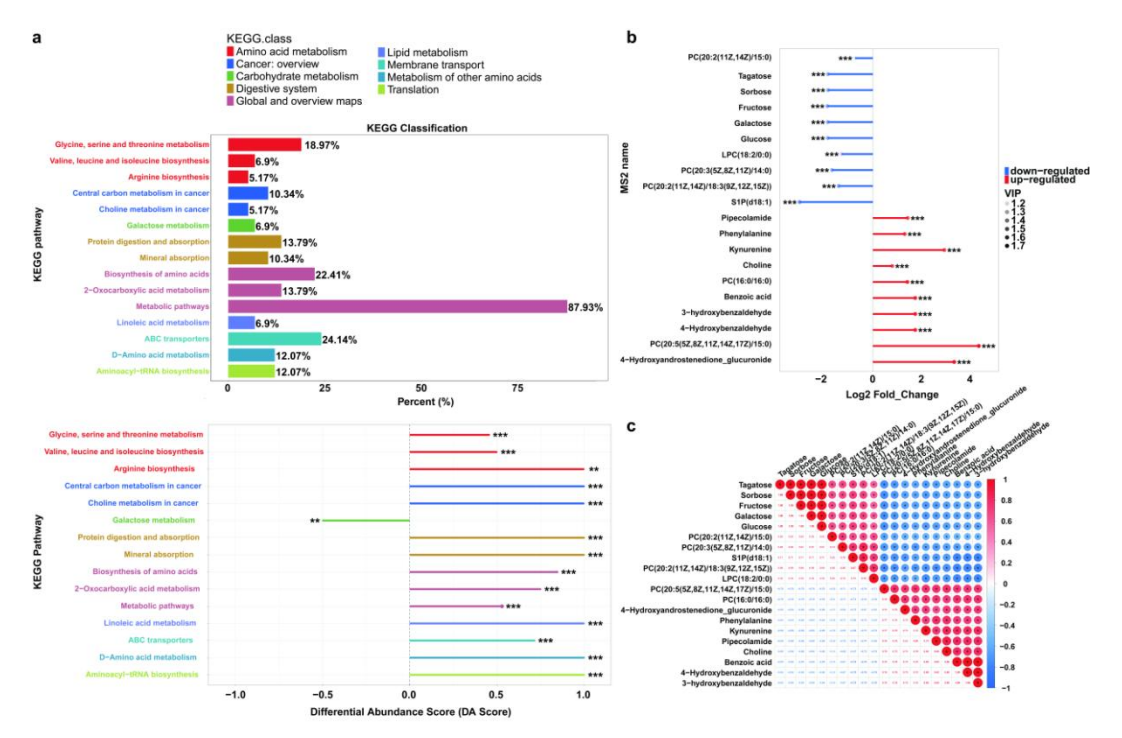
Figure 5 Metabolites selection and model building.

- **a.** Design of the modeling workflow. Random forest algorithm was adopted for feature selection and model training. The 11-PM model was validated in an independent test set. The illustration was created with a full license on BioRender.com.
- **b.** Performance comparison of top 40 machine learning models based on the Area Under the Curve (AUC) scores across both training and testing cohorts. The color gradient, ranging from blue (lower AUC values) to red (higher AUC values), visually represents the performance of each moddel.
- **c.** The relationship between the error rate and the number of trees (Ntree) in a random forest model.
- **d.** Mean decrease accuracy of the eleven metabolites to the 11-PM model.
- **e.** Model performance on training and testing data using Receiver Operating Characteristic (ROC) curves and confusion matrices. A 95% confidence interval was calculated based on the mean and covariance of one thousand random sampling tests.

Supplementary

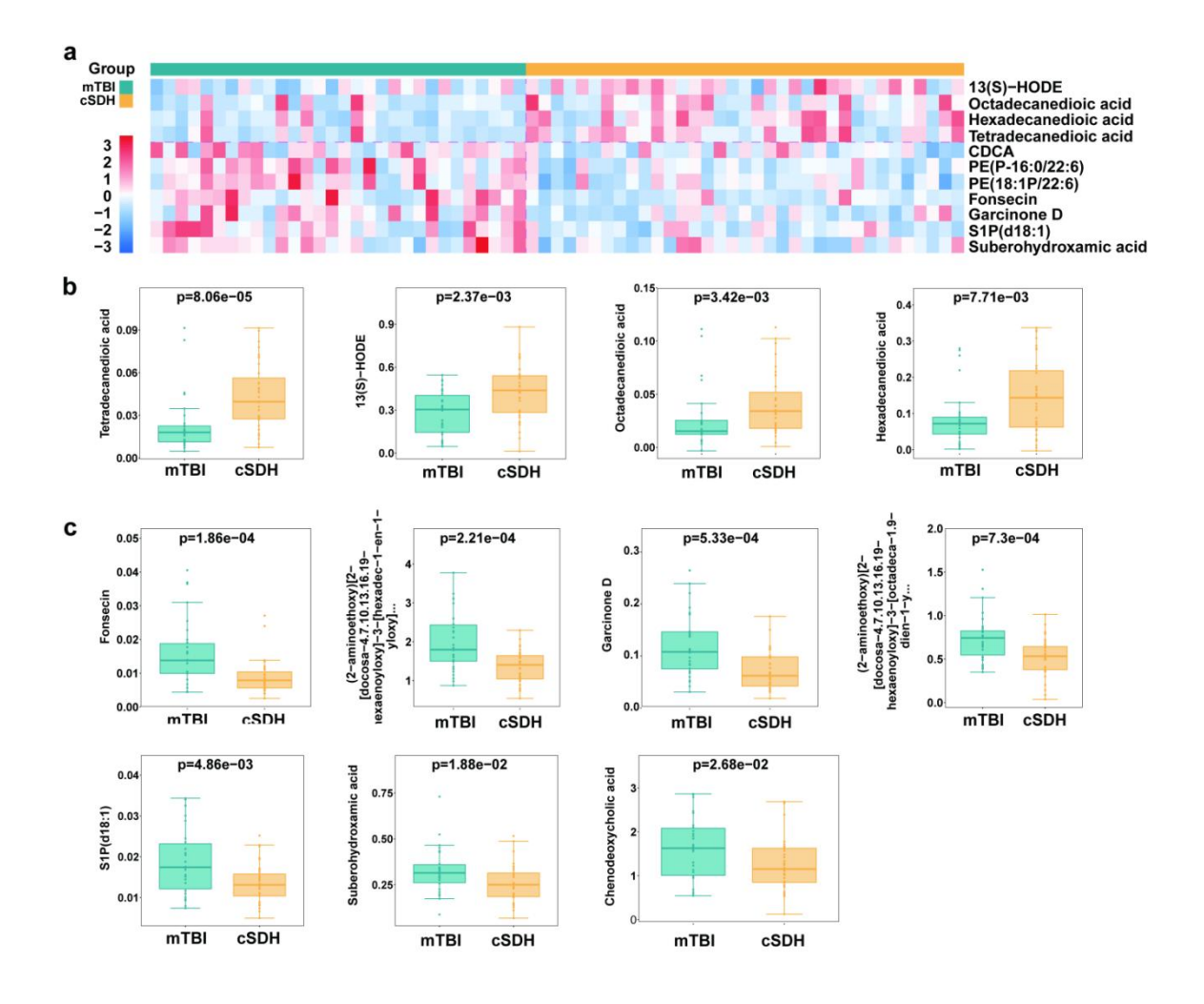


Supplementary figure 1. Heat map illustrating the distinct metabolic profiles of major differential metabolites identified between the peripheral blood and hematoma fluid samples in Cohort 1 of cSDH patients.



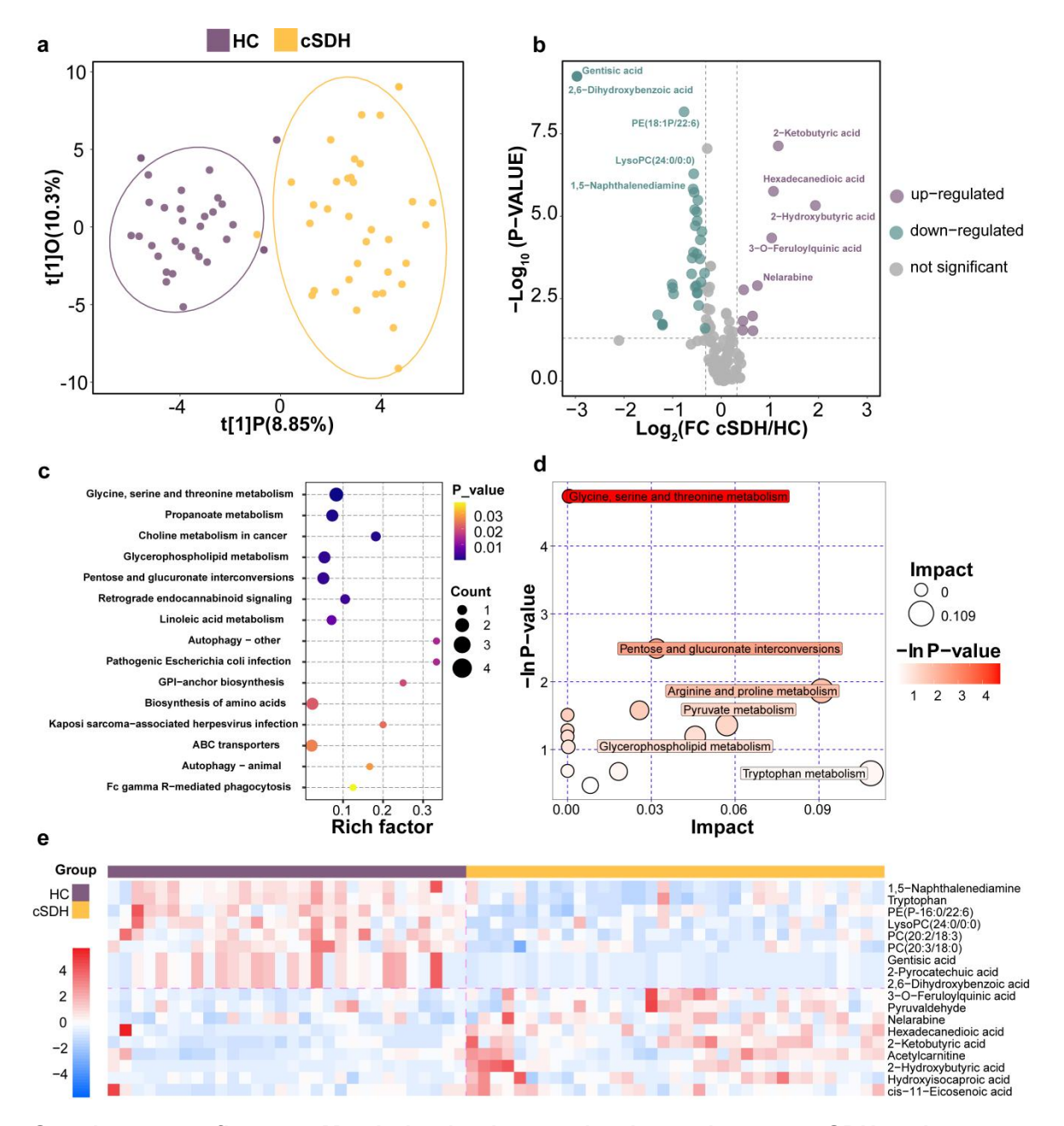
Supplementary figure 2. Metabolic pathway analysis and differential profiling in the cSDH patients.

- a. Kyoto Encyclopedia of Genes and Genomes (KEGG) pathway classification and enrichment analysis of significantly differentially expressed metabolites in the peripheral blood and hematoma fluid of cSDH patients.
- b. Matchstick plot of the top 10 upregulated and downregulated differential metabolites in peripheral blood and hematoma fluid of cSDH patients.
- c. Correlation heatmap of top 10 differential metabolites in peripheral blood and hematoma fluid of cSDH patients. The strength of the relationship between two variables is indicated by the correlation coefficient r. A higher absolute value of r (closer to 1) signifies a stronger association, while a lower absolute value (closer to 0) indicates a weaker association.



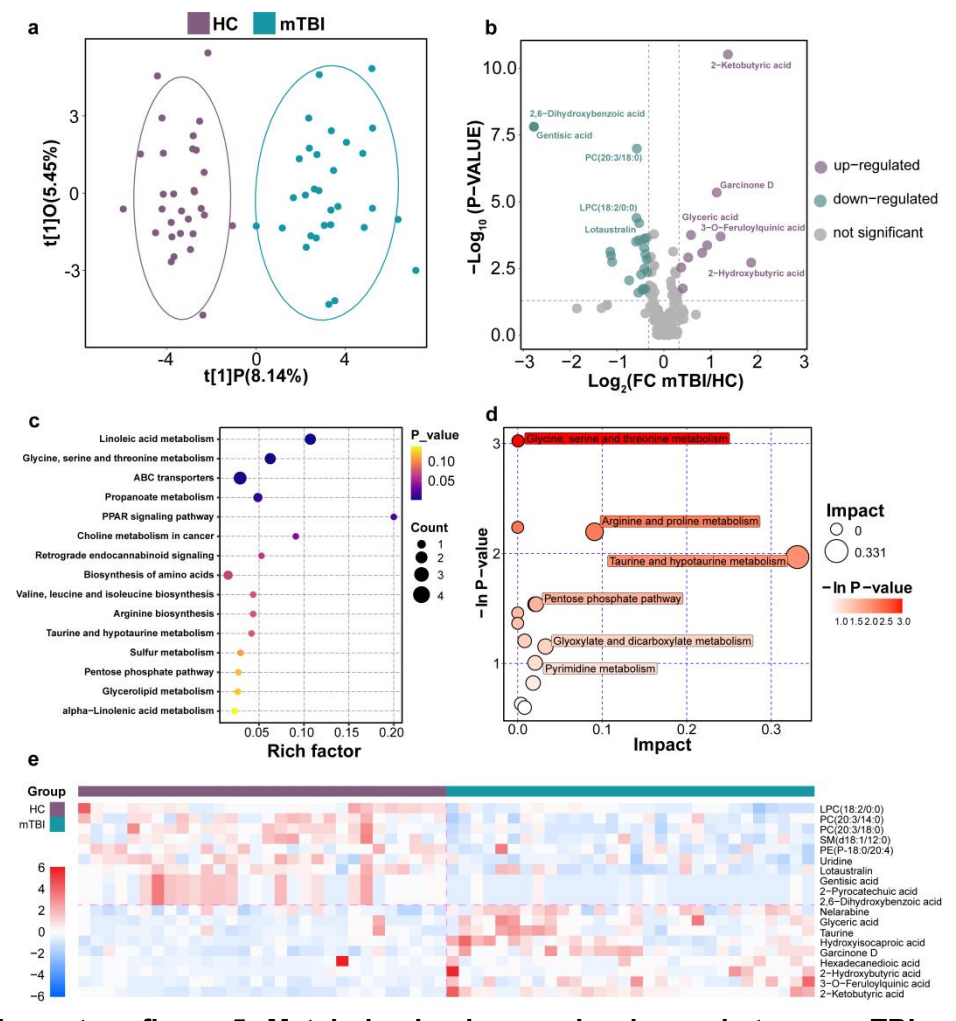
Supplementary figure 3. Significant changes in metabolite levels in patients with cSDH compared to mTBI.

- a. Heat map of major differential metabolites between cSDH and mTBI group in Cohort 1.
- **b.** Box-plots showing significantly elevated levels of four metabolites in cSDH group compared to mTBI group in Cohort 1.
- **c.** Box-plots showing significantly decreased levels of seven metabolites in cSDH group compared to mTBI group in Cohort 1. Each box plot represents the distribution of metabolite concentrations, with the median indicated by the horizontal line within the box, the interquartile range (IQR) represented by the box itself. Statistical significance is indicated by p-values calculated using Student's t-test.



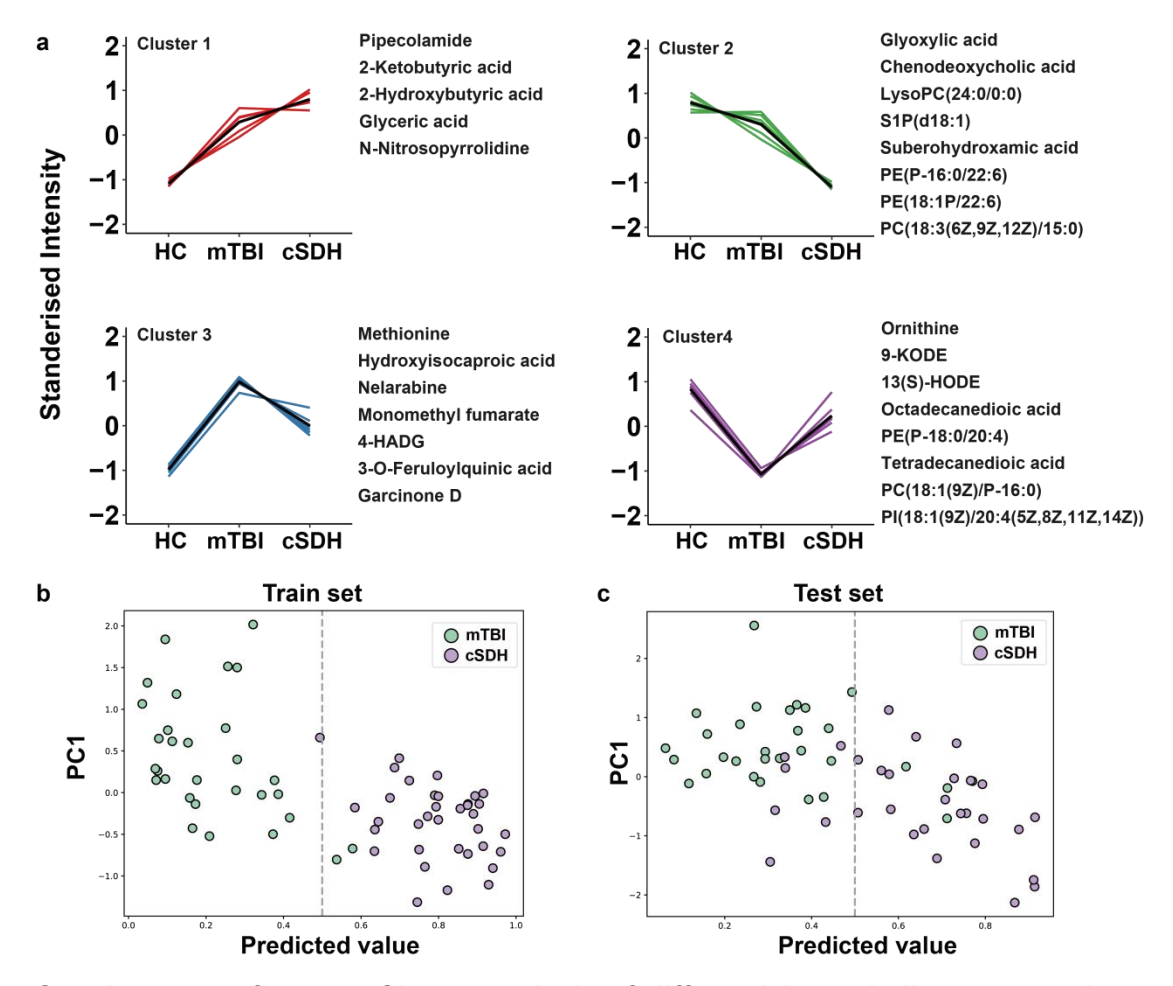
Supplementary figure 4. Metabolomic changes in plasma between cSDH patients and healthy controls.

- **a.** Principal Component Analysis (PCA) of plasma metabolomic profiles in Cohort 1, distinguish cSDH patients (colored in yellow) from healthy controls (colored in purple).
- **b.** Volcano plot of the detected metabolites in metabolomics comparing plasma from cSDH patients and healthy controls. Significantly differential metabolites are colored in purple (upregulated) and green (downregulated); the others are colored in gray.
- **c.** KEGG metabolic pathways enriched by significantly differential metabolites between plasma from cSDH patients and healthy controls.
- **d.** Pathway analysis of significantly differential metabolites between plasma from cSDH patients and healthy controls.
- **e.** Heat map of major differential metabolites between plasma from cSDH patients and healthy controls.



Supplementary figure 5. Metabolomic changes in plasma between mTBI patients and healthy controls.

- **a.** PCA of plasma metabolomic profiles in Cohort 1 demonstrates distinct clustering between mTBI patients (colored in green) and healthy controls (colored in purple).
- **b.** Volcano plot of the detected metabolites in metabolomics comparing plasma samples from mTBI patients and healthy controls. Significantly differential metabolites are colored in purple (upregulated) and green (downregulated); the others are colored in gray.
- **c.** KEGG metabolic pathways enriched by significantly differential metabolites between plasma samples from mTBI patients and healthy controls.
- **d.** Pathway analysis of significantly differential metabolites between plasma samples from mTBI patients and healthy controls.
- **e.** A heat map visualizes the major differential metabolites in plasma samples, distinguishing mTBI patients from healthy controls.



Supplementary figure 6. Cluster analysis of differential metabolites among three groups and the prediction performance of the 11-PM model.

- **a.** Mfuzz clustering of metabolic trajectories using the differential metabolites according to the metabolic changes' similarity in Cohort 2. Representative metabolites of each cluster are presented on the side.
- **b.** The prediction performance of the 11-PM model for distinguishing cSDH (colored in purple) from mTBI (colored in green) in train set.
- **c.** The prediction performance of the 11-PM model for distinguishing cSDH (colored in purple) from mTBI (colored in green) in test set.

Supplementary Table 1	Clinical characteristics of participants			
Characteristics	HC (n=60)	mTBI (n=60)	cSDH (n=65)	p value
Cohort 1				
Number of individuals	30	30	35	
Age,mean±SE	60.6 ± 11.2	62.7 ± 12.7	66.6±13.3	0.347
Gender (m/f)	19/11	22/8	26/9	0.411
PLT	195 ± 45	207 ± 69	219 ± 72	0.372
APTT	25.2 ± 1.8	33.4 ± 6.6	30.7 ± 5.6	<0.0001
PT	11.0 ± 0.8	13.3 ± 1.2	12.8 ± 1.4	<0.0001
Anticoagulant drug history	0/30	0/30	1/34	-
Hypertension	7/23	6/24	7/28	0.817
Injury types:				
Fall	1	17	24	
Accident	1	10	8	
Impact	1	2	1	
Others	1	1	2	
Cohort 2				
Number of individuals	30	30	30	
Age,mean±SE	62.7 ± 10.2	60.6 ± 13.4	65.9±11.8	0.182
Gender (m/f)	20/10	21/9	24/6	0.486
PLT	199±54	199±61	195±72	0.951
APTT	25.1±2.6	30.3±3.2	30.2±4.7	<0.0001
PT	10.9±0.9	12.6±1.0	12.6±1.5	<0.0001
Anticoagulant drug history	0/30	0/30	2/28	-
Hypertension	8/22	10/20	9/21	0.853
Injury types:				
Fall	1	13	21	
Accident	1	13	7	
Impact	1	2	1	
Others	1	2	1	